

Article

Predicting Performance of a District Heat Powered Adsorption Chiller by Means of an Artificial Neural Network

Tomasz Halon ^{1,*} , Ewa Pelinska-Olko ¹ , Malgorzata Szyc ² and Bartosz Zajackowski ¹ 

¹ Faculty of Mechanical and Power Engineering, Wrocław University of Science and Technology, Wyb. Wyspińskiego 27, 50-370 Wrocław, Poland

² Fortum Power and Heat Polska, ul. Antoniego Slonimskiego 1A, 50-304 Wrocław, Poland

* Correspondence: tomasz.halon@pwr.edu.pl; Tel.: +48-7132-041-18

Received: 29 July 2019; Accepted: 27 August 2019; Published: 29 August 2019



Abstract: In this paper, the feasibility of a multi-layer artificial neural network to predict both the cooling capacity and the COP of an adsorption chiller working in a real pilot plant is presented. The ANN was trained to accurately predict the performance of the device using data acquired over several years of operation. The number of neurons used by the ANN should be selected individually depending on the size of the training base. The optimal number of datasets in a training base is suggested to be 35. The predicted cooling capacity curves for a given adsorption chiller driven by the district heating are presented. Predictions of the artificial neural network used show good correlation with experimental results, with the mean relative deviation as low as 1.36%. The character of the cooling capacity curve is physically accurate, and during normal operation for cooling capacities ≥ 8 kW, the errors rarely exceed 1%.

Keywords: adsorption refrigeration; district heat; artificial neural networks

1. Introduction

Combined cooling, heating, and power systems (CCHPs), also called tri-generation systems, have attracted substantial interest during the past few decades. These integrated systems offer high thermal efficiency (compared to single-power generation systems), as well as cost-effective energy with lower environmental impact. The power generation unit produces electric energy and rejects heat as a byproduct. It can be installed locally or remotely (in a co-generation plant). In the latter configuration, the waste heat recovered from the power generator is used to satisfy end user's heating needs through a system of pipes called the district heating network (DH network). The same heat can be used to satisfy consumers' cooling demand by means of thermally-activated refrigeration technologies. Extensive reviews of modern CCHP technologies, conducted by Wu et al. [1] and more recently by Moussawi et al. [2], showed that the majority of the literature on district heating and cooling systems focuses on operational strategies and the optimization of energy conversion technologies. Adsorption cooling systems are described as a promising technology that can utilize low-temperature waste heat [3] or district heat for refrigeration [1], trigeneration [2], or heat upgrade [4].

Artificial neural networks (ANN) offer a modern and systematic approach to complex problems that cannot be described with simple mathematical equations [5,6]. Being able to deal with troublesome databases, incomplete or corrupted by noise signals, ANNs attempt to solve non-linear problems that are too complex to describe mathematically. With access to a sufficient amount of experimental data, it is possible to employ an ANN to learn and model the behavior of almost any type of system. Relying on modern high-speed computing, properly-trained ANNs provide generalizations or discover and predict trends in large datasets.

ANNs have been applied in various fields of engineering, chemistry, medicine, social sciences, etc. Assessing HVAC systems with ANNs started between the end of the 1980s and the beginning of the 1990s [7] in the context of renewable energy systems [8] and cooling load predictions [9]. Modeling of adsorption systems was usually conducted by means of sets of differential equations. The instantaneous solution of energy balances, mass balances, and adsorption kinetics allowed researchers to predict the performance of cooling devices with reasonable accuracy [10]. However, using such models in pilot plant conditions leads to substantial errors because the device is driven by less stable and only partially-predictable energy sources. The prime reason for using ANNs for such cases is their ability to learn from and control complex systems, while relying solely on input and output signals. During problem solving, mathematical equations are substituted with precise numerical solutions that are specific to a particular installation.

Various authors attempted to model thermal systems using ANN algorithms. Kalogirou [8] discussed the use of ANN for modeling of renewable energy systems, including the performance prediction of solar water heating systems, the estimation of heating loads of buildings, the prediction of air flow in a naturally-ventilated test room, etc. [11,12]. Yang [7] discussed the new artificial neural network paradigm applied to thermal problems that cannot be readily solved with traditional approaches. He showed that most of studies focused on ANNs in the context of vapor compression refrigeration systems. The number of works applying ANN algorithms specifically to sorption cooling is limited. The traditional approach to thermodynamic analysis of sorption thermal systems requires multiple analytic functions (differential equations describing components of the system) that need to be solved numerically, which noticeably increases the complexity of the analysis. It makes thermal and refrigeration systems especially suitable for ANN modeling [13].

Mohanraj et al. [14] reviewed the applications of ANN algorithms for energy and exergy analysis of refrigeration, air conditioning, heat pump systems, and sorption devices. Multiple cited papers proved that using ANN to model sorption chillers allows achieving high-performance prediction accuracy. Jani et al. [15] presented a review on the application of ANNs for predicting the performance of solid desiccant cooling systems that are based on the adsorption/desorption principle.

Chow et al. [16] optimized the use of fuel and electricity in a direct-fired absorption chiller system using ANNs and the genetic algorithm. The authors achieved correlation coefficient values for performance of 4.94% with a mean squared error value of 0.00285. Manohar et al. [17], using an ANN and a year's worth of data, were able to predict the COP of an absorption chiller within $\pm 1.2\%$. Labus et al. [18] proposed an inverse ANN model-based control strategy for absorption cooling systems. The results showed that the required cooling load could be achieved with an error of less than 0.05%. Lazrak et al. [19] implemented an ANN to predict outlet temperature and the transferred energy of the driving loop, heat rejection loop, and chilled water loop of a single-effect water–lithium bromide absorption chiller. The absolute relative errors of the transferred energy prediction were 0.1–6.6%.

Hernandez et al. [20] employed an ANN to predict the coefficient of performance of a solar intermittent refrigeration system for ice production under various experimental conditions. Using 658 data points (50/50 split between learning and testing database), the authors were able to achieve high accuracy and reach 0.9875 correlation between the experimental data and the ANN data. Baiju et al. [21] employed ANN for predicting the performance of the adsorbent bed in a solar adsorption refrigeration in terms of the performance index, exergy destruction, uptake efficiency, and exergetic efficiency. The back-propagation algorithm achieved a correlation coefficient of 0.9996 using 105 experimentally-obtained learning data points and 10 testing data points. Frey et al. [22] applied the ANN algorithm to predict the output from an adsorption chiller that was an older model of the device tested in this paper. The authors proved that the ANN process was suitable as an in situ performance test method. The errors were in the range from 2.0–2.8%. The relative deviation of the average COP was in the range from 0.9–0.65%. Krzywanski et al. [23] developed a non-iterative ANN model allowing conducting an optimization study of the silica gel–water adsorption heat pump

with respect to cooling capacity. Using a learning database of 48 data points and a testing database of 10 data points, the maximum relative error made by the algorithm was less than 10%.

The aim of the current work is to test the feasibility of multi-layer ANN to predict both the cooling capacity and the COP of an adsorption chiller with the highest possible accuracy. The ANN was trained using data acquired over several years of operation to predict the performance of the device accurately. Amassed data and results will be later used in the development of a flexible control system, fine-tuned for optimal performance under the conditions and specs of the particular installation, the adsorption chiller, which is a part of the complex heating/cooling system built and operated in Wroclaw, Poland.

In order to confirm the viability of the outputs, the network was tested using both learning and testing databases. The accuracy of predictions was evaluated using the actual output measured at the chiller. The ANN's ability to learn based on various training base sizes was tested in order to estimate the training base size most suitable for the prediction of the chillers' behavior.

2. Artificial Neural Network

The ANN in this study was designed to predict the performance (cooling capacity and COP) of the chiller within the range of source and sink temperatures expected at its installation site. Once trained, the network needed to be able to predict the occurrence of low-performance periods and (in combination with specially-designed control strategies) take necessary steps in order to maximize the performance.

The artificial neural network ANN algorithm was implemented from the nnetdatabase embedded in the R-language environment. The program was written in R Version 3.4.2. It used the nnet database and employed the Fit Neural Network Module (FNNM). The ANN used a back-propagation algorithm, employing four input neurons and one output neuron (see Figure 1).

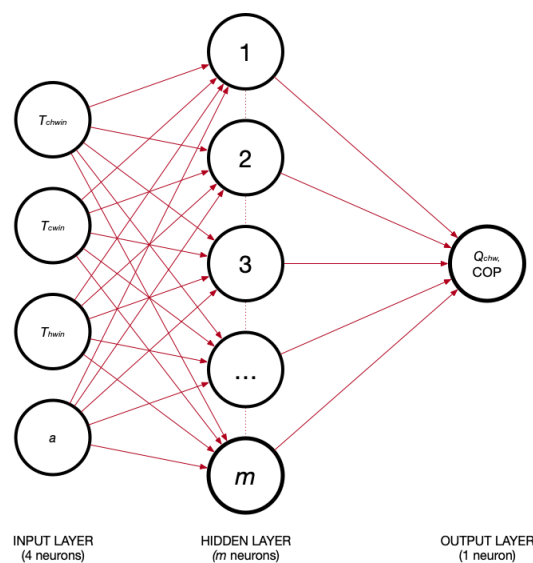


Figure 1. The architecture of the neural network used in the work.

The input neurons were as follow: an ordering parameter a , the inlet temperature of the heating medium T_{hwin} , the inlet temperature of the cooling medium T_{cwin} , and the inlet temperature of chilled water T_{chwin} . The inlet temperatures were the inputs that primarily influenced the cooling capacity and COP. The pilot device was running in real-life conditions, occasionally providing similar sets of input parameters, causing problems during the learning phase. For this reason, the indexing parameter a was the ordering integer assigned to every dataset in the base. It allowed ANN to differentiate between data points clearly and, as a consequence, reduce the number of necessary hidden layer neurons m , decreasing the RMSE and shortening the calculation time. Its value did not influence the calculated

outcome of COP and cooling capacity. As the ordering parameter was not related to other inputs, the ANN recognized skipping it in further iterations.

The presented algorithm used only one output parameter, but the ANN was applied to study two parameters: cooling capacity Q_{chw} and the COP. The network was trained separately for the prediction of each of these parameters.

The number of neurons building up the hidden layer m was systematically evaluated and adjusted during the study in order to increase the accuracy of predictions [24] and the time of predictions [25,26]. Too few neurons yielded under-fitting, but too many neurons resulted in unsatisfactory prediction of new test data that had not been presented in the training process [6]. The exact number of hidden neurons m was chosen by the trial and error method [26]. The accuracy of the network predictions was evaluated by means of selected error functions. In this study, error values were calculated as the root mean square (RMSE), i.e., the maximal absolute error between the experimental and predicted value [6,22].

$$\text{RMSE} = \sqrt{\frac{\sum (y_i - \check{y}_i)^2}{N}} \quad (1)$$

where y_i is the experimentally-obtained value of the tested parameter, \check{y}_i is the value predicted by ANN, and N is the number of experimental data points.

The maximum relative deviation is calculated as follows [6]:

$$E_{max} = \frac{|y_i - \check{y}_i|}{y_i} \quad (2)$$

The training base (TRB) for ANN was a set of data, e.g., from an experiment, organized in a suitable way in order to teach the network to predict results. The TRB covered the entire range of input parameters (temperatures of heating/cooling/cooled mediums). The testing base (TSB) was an additional set of experimental data that served to test the correctness of the results returned by the network. In the analysis presented in this paper, different sizes of TRB and TSB were prepared based on 102 experiments conducted on the chiller within a period of approximately 15 months of normal operation.

Because amassing of experimental data for the TRB required a large number of experiments conducted over a long period of time, it was investigated how sensitive to the size of the TRB the accuracy of prediction was: 35, 55, and 77 data points. The goal was to teach the ANN using the smallest reasonable TRB, so the control system would be able to take over system management as soon as possible.

The number of neurons m should be selected individually, taking into account the required accuracy of the results. For the smallest number of neurons (less than 20), the RMSE values were approximately 2.9–3.0. If the network consisted of more than 20 neurons in the hidden layer, the RMSE dropped to reasonable values from 0.1–0.2.

The optimal number of neurons in a hidden layer m was determined for each analyzed size of the TRB. The analyses presented in the next section always used the optimal number of neurons in the ANN hidden layer. The number of neurons that generated the lowest RMSE: for TRB = 77 was $m = 55$, for TRB = 55 was $m = 35$, and for TRB = 35 was $m = 30$. These three values were used in all the analyses discussed further in this study.

3. Materials and Methods

The outline of the pilot system that was installed and tested in Wrocław is presented in Figure 2, while a photograph is presented in Figure 3. The system was designed to provide cooling for the machine room and for the canteen located in the neighboring building. The adsorption chiller was driven with heat supplied from the district heating or by the solar collectors mounted on the roof of the building. The driving temperature depended on the actual operating conditions of the heating network, while the cooling load was determined by the consumer.

The adsorption chiller was an integrated type (patented and commercialized by Fahrenheit AG) with silica gel and water as the working pair. The device consisted of two vacuum-tight compartments that enclosed both an adsorption bed and a heat exchanger, so it did not require any valves working in the vacuum conditions. Its maximum electricity consumption was 756 W according to the producer.

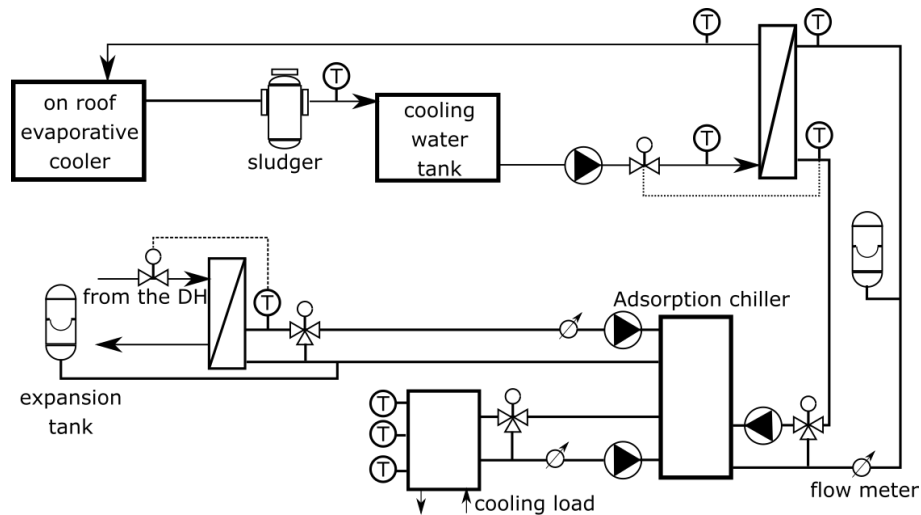


Figure 2. Schematics of the installation for testing the adsorption chiller driven by heat from the DH network.

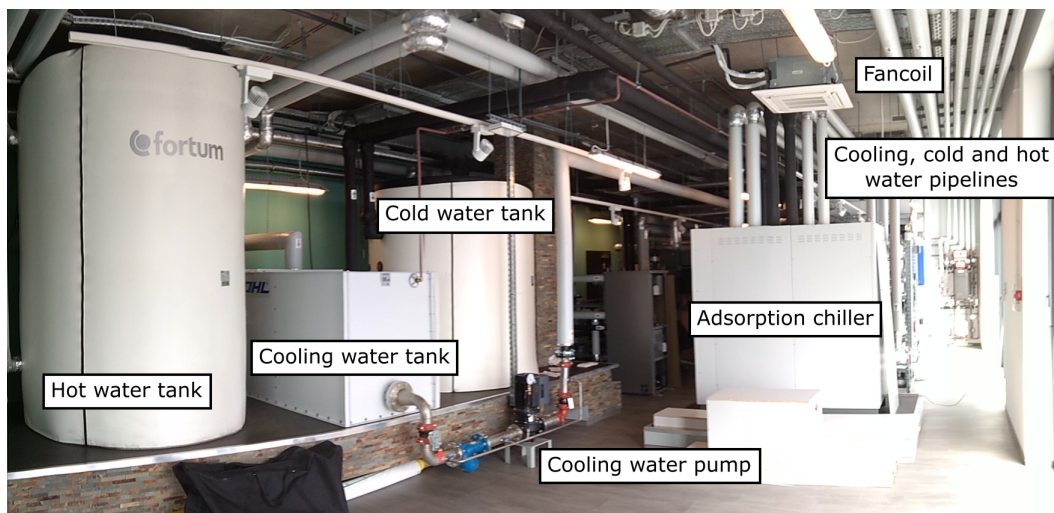


Figure 3. The whole system with the adsorption chiller, pipelines, and storage vessels for cooling, hot and chilled water.

Chilled water was stored in a 3-m³ insulated tank working as a cold reservoir and compensation for chilled water temperature variation produced by the cyclic work of the adsorption chiller. For the experimental purposes, chilled water temperature could be increased by a heat exchanger with DH water.

Heating water came from the DH network. Its temperature usually was set by the outside conditions. For the city of Wrocław, it was around 65 °C in summer. Due to the possibility of changing the flow through the heat exchanger between the system and DH, the heating water temperature could be decreased down to 55 °C. If needed, the heating water temperature could be increased by the solar collectors. The hot water from solar collectors was stored in a 4-m³ insulated tank.

The cooling water released heat in a cooling tower on the roof of the building. It was open, so the dirt from the air could block the chillers' heat exchanger. Because of that, the cooling circuit was divided into two. The part with the cooling tower had a 1.1-m³ tank. Cooling water temperature could be adjusted by throttling the flow of water on the cooling tower side of the circuit.

The pumps and switches were controlled by computer software that was able to adjust the duration of the adsorption/desorption phase in order to maximize cooling capacity. In order to reduce the noise level and decrease the number of variables for the ANN training, for experiments discussed in this study, the length of adsorption/desorption phase was fixed at 900 s.

Measurement Uncertainty

Data acquisition was done with a time interval of 15 s. Inlet and outlet chilled and cooling water temperature, outlet hot water temperature, and the temperatures of all heat exchangers were measured from the device level by the PT-1000 sensor. Hot water inlet temperature T_{hwin} was measured with a PT-500 sensor on the pipeline from the chiller. All temperature sensors were A class ($\pm 0.15 + 0.002 \cdot T$). The cooling water mass flow rate \dot{m}_{cw} and heating water mass flow rate \dot{m}_{hw} were measured with an ULTRAFLOW 54 ultrasonic flow meter at 4% uncertainty.

The adsorption chiller worked in cycles and remained in unsteady conditions. Because of that, all data points for learning and testing of the ANN were medium values determined for a single operating cycle. Cooling capacity was calculated every 15 s, and then, the average was calculated for the whole cycle. The COP was calculated from the averaged cooling capacity and heating power.

The uncertainty of averaged heating power and cooling capacity was calculated using the partial derivatives method. The standard deviation was neglected due to the unsteady conditions.

The uncertainty of heating power ranged from 5–9% depending on the value, while the uncertainty of cooling capacity ranged from 5–34%. The highest uncertainty was observed for the worst working conditions, where the cooling capacity was below 1 kW. For standard working conditions, it never exceeded 13%. The uncertainty of the COP was less than 1%.

4. Results and Discussion

4.1. ANN Performance Prediction Accuracy

The quality of the ANN predictions depended on the number of neurons on a hidden layer and on the size of the TRB. Once the network was trained using the amassed experimental data, the ANN was used to predict cooling capacity and the coefficient of performance of the chiller. The algorithm was trained using three different TRBs and then tested on the entire experimental dataset (102 data points). The comparison of experimental and predicted results is presented in Figure 4. The size of the hidden layer was set to minimize RMSE properly. The values of selected cooling capacities measured experimentally (averaged) and predicted by ANN are shown in Table 1.

Table 1. Accuracy of ANN predictions for ten selected cooling capacities (out of 102).

$Q_{chw,exp}$ kW	$Q_{chw,ANN-35}$ kW	$E_{max,35}$ %	$Q_{chw,ANN-55}$ kW	$E_{max,55}$ %	$Q_{chw,ANN-77}$ kW	$E_{max,77}$ %
3.5991	3.6781	2.20	3.5413	1.61	3.5685	1.07
4.2995	4.2968	0.06	4.2310	1.59	4.3129	0.31
5.0480	5.0458	0.04	5.1188	1.40	5.0546	0.13
6.3266	6.2997	0.43	6.2785	0.76	6.2409	1.36
6.9407	7.1588	3.14	7.00	0.87	7.0529	1.62
8.3077	8.1042	2.45	8.1497	1.90	8.1913	1.40
8.8355	8.8122	0.83	8.7362	1.68	8.7346	1.70
9.1887	9.2120	0.25	9.1738	0.16	9.1884	0.00
10.1070	10.0394	0.67	10.0422	0.64	9.9974	1.08
11.0533	11.0093	0.40	11.0724	0.17	11.0708	0.16

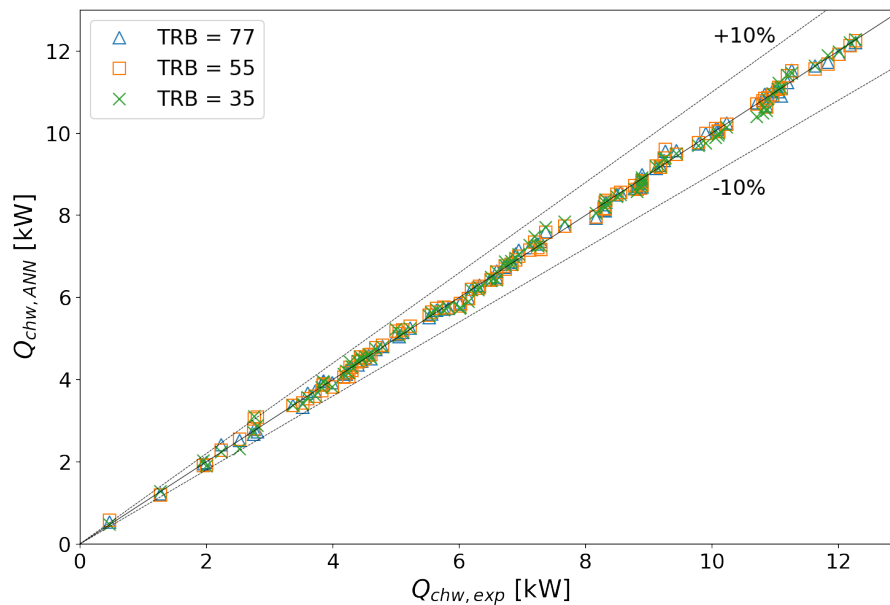


Figure 4. Comparison of predicted and measured cooling capacities.

The accuracy of predictions evaluated as the relative average deviation tended to decrease with an increasing size of TRB: $E_{max,35,avg} = 1.63\%$, $E_{max,55,avg} = 1.70\%$, and $E_{max,77,avg} = 1.36\%$. The maximum error registered for an individual data point 26.52% was registered for the edge of the operating range at the lowest measured cooling capacity 0.47 kW. During normal operation for cooling capacities ≥ 8 kW, the relative errors rarely exceeded 1% (see Figure 4 and Table 1). The average absolute deviation was 0.098, 0.084, and 0.077 for the TRB = 35, 55, and 77, respectively.

The same principles can be used to predict the COP. Using an identical number of neurons in a hidden layer as in the example above, the algorithm was trained to predict the COP of the device. The results of comparison of the experimental and calculated values are shown in Figure 5.

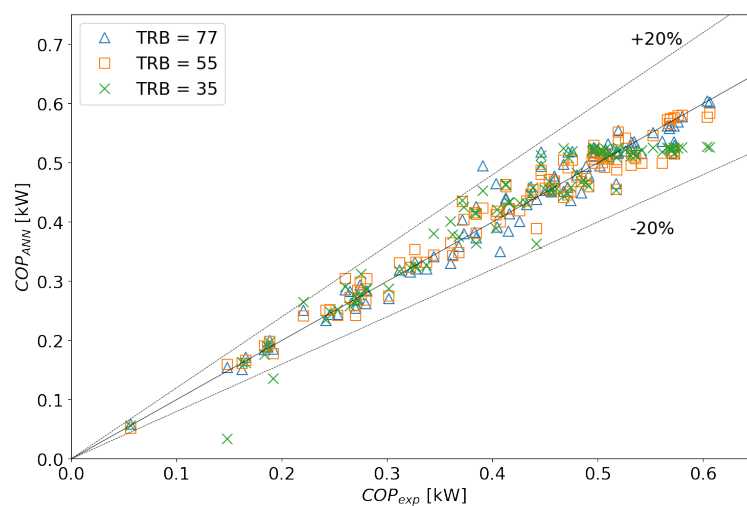


Figure 5. Comparison of predicted and measured coefficients of performance.

The discrepancies and substantially larger errors could be explained by the much more noisy and less predictable behavior of the device. The COP was calculated as the ratio between the cooling capacity and the heating capacity of the DH network. In pilot conditions, the latter was less controllable, which led to more noise and inaccuracies.

The accuracy of COP predictions evaluated as a relative average deviation tended to decrease with the increasing size of TRB, but the values were much higher than in the case of cooling capacities: $E_{max,35,avg} = 6.31\%$, $E_{max,55,avg} = 4.64\%$, and $E_{max,77,avg} = 4.34\%$. The maximum error registered for an individual data point was up to 26.52% (the point standing out in Figure 5 and Table 2). The average absolute deviation was 0.024, 0.018, and 0.017 for TRB = 35, 55, and 77, respectively.

Table 2. Accuracy of ANN predictions for ten selected coefficients of performance (out of 102).

COP_{exp}	COP_{ANN-35}	$E_{max,35}$ %	COP_{ANN-55}	$E_{max,55}$ %	COP_{ANN-77}	$E_{max,77}$ %
0.1655	0.1718	3.75	0.1664	0.53	0.1616	2.40
0.1883	0.1996	5.97	0.1984	5.33	0.1960	4.05
0.2647	0.2827	6.80	0.2727	2.84	0.2575	2.72
0.3261	0.3315	1.64	0.3534	8.35	0.3239	0.67
0.3909	0.4946	26.52	0.4233	8.28	0.4522	15.59
0.4072	0.3500	14.03	0.4003	1.69	0.4159	2.12
0.4586	0.4773	4.08	0.4687	2.20	0.4594	0.18
0.4910	0.4796	2.31	0.4590	6.51	0.4603	6.24
0.5342	0.5354	0.21	0.5098	4.56	0.5169	3.23
0.5721	0.5350	6.49	0.5209	8.95	0.5241	8.39

The cooling capacity could be predicted with reasonable accuracy based on a small number of experimental data points. In order to achieve similar accuracy of COP predictions, a substantially bigger experimental database is required, which is not always possible.

4.2. Cooling and Chilled Water Temperature Effect on Cooling Capacity and COP

The characteristics shown on Figure 6 were predicted by the ANN for a cooling water temperature range typical for the Polish climate. The hot water temperature was 65 °C, as it was the most common value occurring during the experiments. The adsorption chillers' cooling capacity Q_{chw} decreased with increasing the cooling water temperature. Higher cooling water temperature meant a higher adsorption temperature, which led to lower adsorbent uptake. Lower adsorbent uptake decreased the sorption capacity of the bed and, so, the mass of the refrigerant in the evaporator, leading to lower cooling capacity.

The higher the chilled water inlet temperature T_{chwin} , the higher the cooling capacity Q_{chw} . This is because the chilled water inlet temperature increased the evaporation pressure. At constant adsorption temperature, it led to a higher adsorption capacity of the bed and higher cooling capacity.

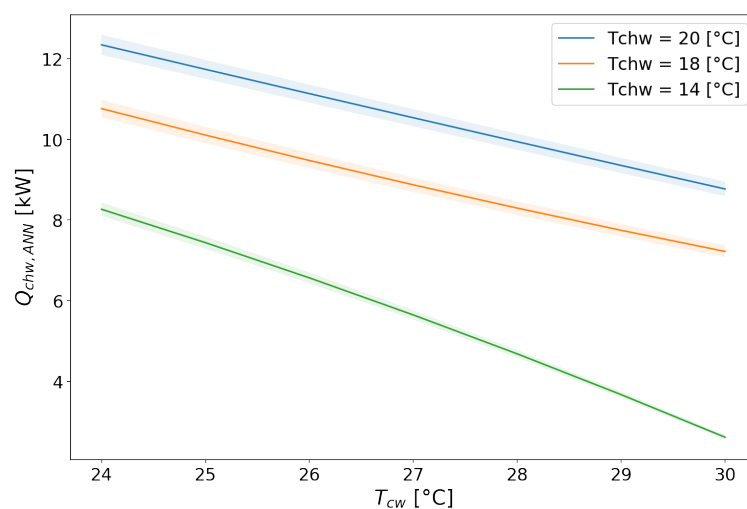


Figure 6. Influence of cooling water temperature on cooling capacity.

At chilled water inlet temperature $T_{chwin} = 20\text{ }^{\circ}\text{C}$ and hot water temperature $T_{hwin} = 65\text{ }^{\circ}\text{C}$, the cooling capacity Q_{chw} decreased by 28% when the cooling water temperature was increased from 24–30 $^{\circ}\text{C}$ (from 12.3–8.9 kW, respectively). At chilled water inlet temperature $T_{chwin} = 14\text{ }^{\circ}\text{C}$, the cooling capacity Q_{chw} decreased to 2.9 kW when the cooling water temperature was 30 $^{\circ}\text{C}$.

At $T_{hwin} = 65\text{ }^{\circ}\text{C}$ and $T_{cwin} = 24\text{ }^{\circ}\text{C}$, the predicted cooling capacity Q_{chw} dropped by 35% at the lowest chilled water inlet temperature compared to the highest one (12.3–8 kW for 14–20 $^{\circ}\text{C}$, respectively).

4.3. Heating Water Temperature Effect on Cooling Capacity and COP

The characteristics shown on Figure 7 were predicted by the ANN for a hot water temperature range typical for district heating. The cooling water temperature was 27 $^{\circ}\text{C}$. The increase of hot water inlet temperature increased the cooling capacity Q_{chw} of an adsorption chiller. At chilled water inlet temperature $T_{chwin} = 14\text{ }^{\circ}\text{C}$, the cooling capacity Q_{chw} was 65% smaller for the hot water temperature $T_{hwin} = 55\text{ }^{\circ}\text{C}$ than at 75 $^{\circ}\text{C}$ (2.6 and 7.4 kW, respectively). At $T_{chwin} = 20\text{ }^{\circ}\text{C}$ and $T_{hwin} = 55\text{ }^{\circ}\text{C}$, the cooling capacity Q_{chw} was 23% smaller than at $T_{hwin} = 75\text{ }^{\circ}\text{C}$ (8.9 and 11.6 kW, respectively).

This was due to the fact, that the increase of regeneration temperature increased the sorption capacity of the bed. Desorption that took place at higher temperatures meant that less refrigerant would stay on the sorbent, i.e., the silica gel would be drier. During adsorption, it would be able to take more refrigerant vapor, so more refrigerant would evaporate in the evaporator (the cooling capacity of the evaporator would be higher).

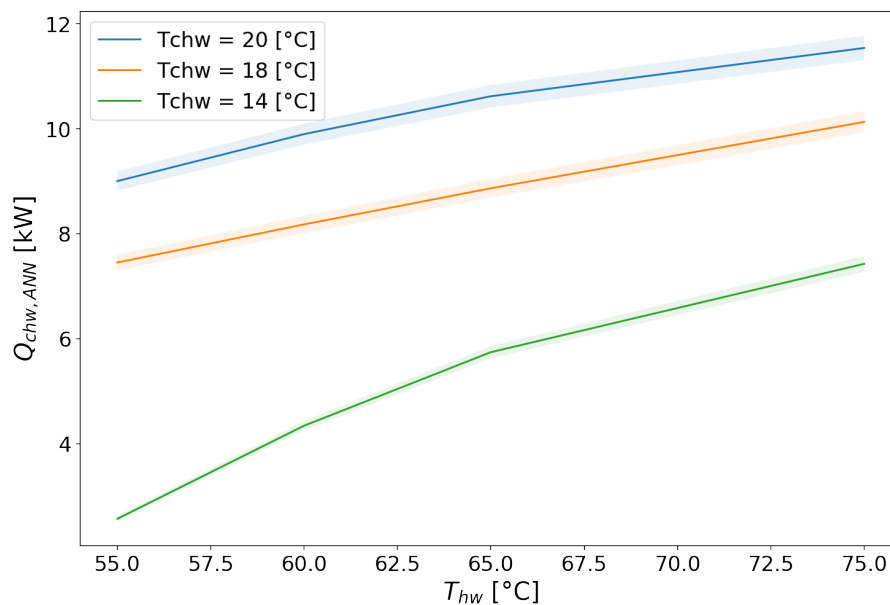


Figure 7. Influence of heating water temperature on cooling capacity.

5. Conclusions

In the paper, it was shown that the ANNs could be successfully used to learn from and predict the performance of an adsorption chiller.

For the highest accuracy, the number of hidden neurons m should be selected individually depending on the size of the training base, taking into account the required accuracy of the results. For the smallest number of neurons (less than 20), the root mean squared error (RMSE) values were approximately 2.9–3.0. If the network consisted of more than 20 neurons in the hidden layer, the RMSE dropped to a reasonable 0.1–0.2.

The number of neurons that generated the lowest RMSE was for $\text{TRB} = 77$, $m = 55$; for $\text{TRB} = 55$, $m = 35$; and for $\text{TRB} = 35$, $m = 30$. The accuracy of predictions evaluated as the average of

maximum errors decrease with an increasing size of the TRB: $E_{max,35,avg} = 1.63\%$, $E_{max,55,avg} = 1.70\%$, and $E_{max,77,avg} = 1.36\%$.

According to the ANNs' prediction, cooling capacity Q_{chw} decreased with increasing cooling water temperature, while for the increased chilled water inlet temperature T_{chwin} and hot water inlet temperature T_{hwin} , it increased. It remained consistent with the fundamental operating principles of adsorption systems and with the experimental data. Predictions of the ANN showed good correlation with experimental results obtained in a real pilot plant. The character of the cooling capacity curve was physically accurate, and during normal operation for cooling capacities ≥ 8 kW, the relative errors rarely exceeded 1%.

The behavior of an adsorption chiller (its cooling capacity) can be predicted with reasonable accuracy based on a small number of experimental data points. In order to achieve similar accuracy of COP predictions, a substantially bigger experimental database is required, which is not always possible ($E_{max,35,avg} = 6.31\%$, $E_{max,55,avg} = 4.64\%$ and $E_{max,77,avg} = 4.34\%$).

Author Contributions: Conceptualization, T.H. and B.Z.; methodology, T.H. and E.P.-O.; software, E.P.-O.; validation, T.H. and E.P.-O.; formal analysis, E.P.-O.; investigation, T.H.; resources, T.H. and M.S.; data curation, T.H. and E.P.-O.; writing, original draft preparation, T.H. and E.P.-O.; writing, review and editing, B.Z. and M.S.; visualization, B.Z.; supervision, M.S.; project administration, T.H.; funding acquisition, B.Z.

Funding: This publication was prepared in collaboration with Fortum Power and Heat Poland, which financed research works necessary to prepare this publication under Contract No. 01/08/2018 (U/0180/343/2018).

Conflicts of Interest: The authors declare no conflict of interest. The funders had no role in the design of the study; in the collection, analyses, or interpretation of the data.

Abbreviations

The following abbreviations are used in this manuscript:

ANN	Artificial neural network
COP	Coefficient of performance
TRB	Training base
TSB	Testing base
RMSE	Root mean square error

References

1. Wu, D.; Wang, R. Combined cooling, heating and power: A review. *Prog. Energy Combust. Sci.* **2006**, *32*, 459–495. [[CrossRef](#)]
2. Al Moussawi, H.; Fardoun, F.; Louahli-Gualous, H. Review of tri-generation technologies: Design evaluation, optimization, decision-making, and selection approach. *Energy Convers. Manag.* **2016**, *120*, 157–196. [[CrossRef](#)]
3. Ommen, T.; Markussen, W.B.; Elmegaard, B. Lowering district heating temperatures—Impact to system performance in current and future Danish energy scenarios. *Energy* **2016**, *94*, 273–291. [[CrossRef](#)]
4. Aristov, Y.I. Adsorption Dynamics in Adsorptive Heat Transformers: Review of New Trends. *Heat Transf. Eng.* **2014**, *35*, 1014–1027. [[CrossRef](#)]
5. Hou, Z.; Lian, Z.; Yao, Y.; Yuan, X. Cooling-load prediction by the combination of rough set theory and an artificial neural-network based on data-fusion technique. *Appl. Energy* **2006**, *83*, 1033–1046. [[CrossRef](#)]
6. Hosoz, M.; Ertunc, H.M.; Bulgurcu, H. Performance prediction of a cooling tower using artificial neural network. *Energy Convers. Manag.* **2007**, *48*, 1349–1359. [[CrossRef](#)]
7. Yang, K. Artificial Neural Networks (ANNs): A New Paradigm for Thermal Science and Engineering. *J. Heat Transf.* **2008**, *130*, 093001. [[CrossRef](#)]
8. Kalogirou, S.A. Artificial neural networks in renewable energy systems applications: A review. *Renew. Sustain. Energy Rev.* **2001**, *5*, 373–401. [[CrossRef](#)]
9. Abbassi, A.; Bahar, L. Application of neural network for the modeling and control of evaporative condenser cooling load. *Appl. Therm. Eng.* **2005**, *25*, 3176–3186. [[CrossRef](#)]
10. Teng, W.S.; Leong, K.C.; Chakraborty, A. Revisiting adsorption cooling cycle from mathematical modelling to system development. *Renew. Sustain. Energy Rev.* **2016**, *63*, 315–332. [[CrossRef](#)]

11. Kassai, M.; Simonson, C.J. Performance investigation of liquid-to-air membrane energy exchanger under low solution/air heat capacity rates ratio conditions. *Build. Serv. Eng. Res. Technol.* **2015**, *36*, 535–545. [[CrossRef](#)]
12. Kassai, M. Experimental investigation of carbon dioxide cross-contamination in sorption energy recovery wheel in ventilation system. *Build. Serv. Eng. Res. Technol.* **2018**, *39*, 463–474. [[CrossRef](#)]
13. Sun, D.W. Thermodynamic design data and optimum design maps for absorption refrigeration systems. *Appl. Therm. Eng.* **1997**, *17*, 315–332. [[CrossRef](#)]
14. Mohanraj, M.; Jayaraj, S.; Muraleedharan, C. Applications of artificial neural networks for refrigeration, air-conditioning and heat pump systems—A review. *Renew Sustain. Energy Revs* **2012**, *16*, 1340–1358. [[CrossRef](#)]
15. Jani, D.; Mishra, M.; Sahoo, P. Application of artificial neural network for predicting performance of solid desiccant cooling systems—A review. *Renew. Sustain. Energy Rev.* **2017**, *80*, 352–366. [[CrossRef](#)]
16. Chow, T.; Zhang, G.; Lin, Z.; Song, C. Global optimization of absorption chiller system by genetic algorithm and neural network. *Energy Build.* **2002**, *34*, 103–109. [[CrossRef](#)]
17. Manohar, H.; Saravanan, R.; Renganarayanan, S. Modelling of steam fired double effect vapour absorption chiller using neural network. *Energy Convers. Manag.* **2006**, *47*, 2202–2210. [[CrossRef](#)]
18. Labus, J.; Hernández, J.; Bruno, J.; Coronas, A. Inverse neural network based control strategy for absorption chillers. *Renew. Energy* **2012**, *39*, 471–482. [[CrossRef](#)]
19. Lazrak, A.; Boudehenn, F.; Bonnot, S.; Fraisse, G.; Leconte, A.; Papillon, P.; Souyri, B. Development of a dynamic artificial neural network model of an absorption chiller and its experimental validation. *Renew. Energy* **2016**, *86*, 1009–1022. [[CrossRef](#)]
20. Hernández, J.; Rivera, W.; Colorado, D.; Moreno-Quintanar, G. Optimal COP prediction of a solar intermittent refrigeration system for ice production by means of direct and inverse artificial neural networks. *Sol. Energy* **2012**, *86*, 1108–1117. [[CrossRef](#)]
21. Baiju, V.; Muraleedharan, C. Artificial neural network modelling of adsorbent bed in a solar adsorption refrigeration system. *Proc. Inst. Mech. Eng. Part C* **2013**, *227*, 346–358. [[CrossRef](#)]
22. Frey, P.; Fischer, S.; Drück, H. Artificial Neural Network modelling of sorption chillers. *Sol. Energy* **2014**, *108*, 525–537. [[CrossRef](#)]
23. Krzywanski, J.; Grabowska, K.; Herman, F.; Pyrka, P.; Sosnowski, M.; Prauzner, T.; Nowak, W. Optimization of a three-bed adsorption chiller by genetic algorithms and neural networks. *Energy Convers. Manag.* **2017**, *153*, 313–322. [[CrossRef](#)]
24. Eldracher, M. Classification of Non-Linear-Separable Real-World-Problems Using Delta-Rule, Perceptrons, and Topologically Distributed Encoding. In *Applied Computing: Technological Challenges of the 1990's, Proceedings of the 1992 ACM/SIGAPP Symposium on Applied Computing, Kansas City, MO, USA, 1–3 March 1992*; ACM Press: New York, NY, USA, 1992; pp. 1098–1104.
25. Cantú-Paz, E. Pruning Neural Networks with Distribution Estimation Algorithms. In *Proceedings of the Genetic and Evolutionary Computation (GECCO 2003), Chicago, IL, USA, 12–16 July 2003*; pp. 790–800.
26. Pavlidis, N.G.; Tasoulis, O.K.; Plagianakos, V.P.; Nikiforidis, G.; Vrahatis, M.N. Spiking neural network training using evolutionary algorithms. In *Proceedings of the International Joint Conference on Neural Networks, Montreal, QC, Canada, 31 July–4 August 2005; Volume 4*, pp. 2190–2194.

